

# Assessing Future Precipitation in Gandaki River Basin based on CMIP6 Projections

Bibek Thapa <sup>a</sup>, Vishnu Prasad Pandey <sup>a</sup>, Rocky Talchabhadel <sup>b</sup>

<sup>a</sup> Department of Civil Engineering, Pulchowk Campus, IOE, Tribhuvan University, Nepal

<sup>b</sup> Texas A&M AgriLife Research, Texas A&M University, El Paso, TX, USA

**Corresponding Email:** <sup>a</sup> email.bibekthapa@gmail.com

## Abstract

Selecting representative climate models and appropriate bias correction techniques is a decisive step for assessing climate change. A widely used approach for selecting climate models is the evaluation of past performance during the historical period. The selected models are then used to assess the likely deviation in the future under changing climate. The multimodel ensemble of the selected global climate models (GCMs) helps to reduce associated uncertainties in projection. This study included a pool of twelve GCMs, from the Coupled Model Inter-comparison Project - Phase 6 (CMIP6) under two shared socioeconomic pathways, SSP245 and SSP585, to assess projected change in precipitation in the Gandaki River Basin. Future precipitation is projected based on four selected CMIP6-GCMs (i.e., EC-Earth3-Veg, MPI-ESM1-2-HR, MPI-ESM1-2-LR, EC-Earth3) and their ensemble, using robust quantile mapping method for three future periods, namely, near (NF: 2021-2046), mid (MF: 2047-2073), and far (FF: 2074-2100). The precipitation projection from the multimodel ensemble indicated a 7-32% increase in annual precipitation in the NF and 18-45% increase in the FF under SSP245, while 6-35% increase in the NF and 42-110% increase in the FF under SSP585 with respect to the baseline period (1980-2014). Under both scenarios, future precipitation is projected to decrease from November to March and increase from April to October. In terms of season, it is projected to increase during pre-monsoon and monsoon seasons and decrease in post-monsoon and winter seasons under both scenarios. Our study highlights that the variation in the rate of increase is higher towards the FF, and the severity of the increase is more pronounced under SSP585.

## Keywords

Bias correction method, climate change, Gandaki basin, global climate model, precipitation projection

## 1. Introduction

The fifth assessment report (AR5) of the Intergovernmental Panel on Climate Change (IPCC) describes the technological, scientific, economic, and social aspects of climate change [1]. The report stated that the risks associated with freshwater under changing climate might increase as the greenhouse gas (GHG) concentration in the atmosphere rises due to accelerated anthropogenic activities. River basins across the globe are experiencing varying degrees of impact from climate change [2, 3, 4]. IPCC has defined a set of Shared Socioeconomic Pathways/Representative Concentration Pathways (SSP/RCP) based scenarios under different warming scenarios for Phase 6 of Coupled Model Inter-comparison Project (CMIP6) for future climate projections [5]. Precipitation is one of the key

parameters of the climate and the hydrologic cycle. Therefore, understanding future precipitation projection is important for assessing the impact of climate change on hydrology.

For the projection of future water availability, a reliable projection of future climate (temperature and precipitation) is an essential first step. Studies have been carried out to project the future climate in local basins and its possible implications on hydrology. For example, Rajbhandari et al. [6] projected precipitation and temperature patterns in the Koshi river basin for RCP4.5 and RCP8.5 scenarios. Khadka et al. [7] studied the impact of climate change on the snow hydrology of the Koshi river basin. Dahal et al. [8] and Pandey et al. [9, 10] estimated the impact of climate change on water availability in Bagmati, Chamelia, and Karnali-Mohana basins. These studies

projected considerable change in the hydrology of the local basin in the long run due to climate change under different future scenarios.

Most of the comprehensive studies on future climate projection have been carried on the Koshi River basin [6, 11, 12], Bagmati River basin [8], Karnali River basin [10] and studies conducted previously are based on results of Phase-3 and Phase-5 of Coupled Model Inter-comparison Project (CMIP) model outputs (i.e., CMIP3 or CMIP5). CMIP6 is the latest generation of future climate models, and there are limited studies based on the latest climate models. However, few studies [13, 14] highlight the use of CMIP6 precipitation to assess projected extreme precipitation. This study projects basin-wide future precipitation in the Gandaki River basin (GRB) based on the CMIP6 model outputs.

This paper aims at: (a) selection of a suitable set of CMIP6 Global Circulation Models (GCMs) for the GRB, (b) selection of the best-suited method for correcting biases in climate model outputs, and (c) projection of future precipitation based on an ensemble of the selected GCMs and the best-suited bias correction method.

## 2. Study Area

The GRB is a transboundary basin extending from China in the north, through Nepal, to India in the south with a total drainage area of 46,300 km<sup>2</sup> at the confluence with the Ganges. Of the total area 72% lies in Nepal (Figure 1), 18% in India, and 10% in China. Within Nepal, the GRB is bounded by the Karnali basin to the west and the Koshi basin to the east.

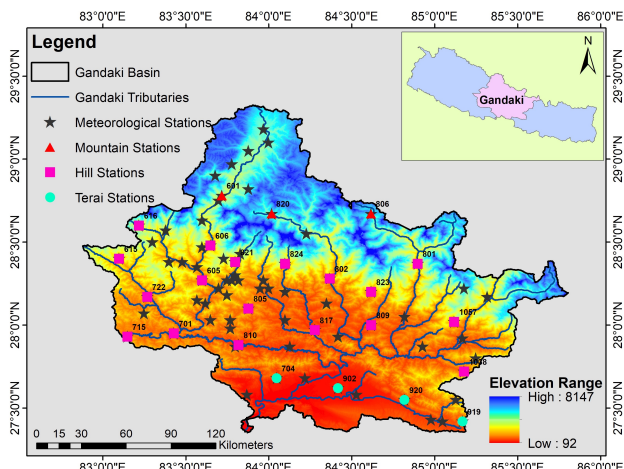


**Figure 1:** Location and associated details of the Gandaki River Basin

The catchment area of the Gandaki basin at Devghat is 31,100 km<sup>2</sup>. The Gandaki River is known as the Narayani within Nepal and as the Gandak in India, where it joins the Ganges. The GRB has a wide spatial heterogeneity in topography and climate, with topographical variation ranging from 92 to 8,147 m above mean sea level. The average annual precipitation varies from as low as 150 mm in Trans-Himalayas to as high as 5400 mm in the hilly region.

### **3. Methodology and Data**

The methodological flow chart of the study is given in Figure 2.

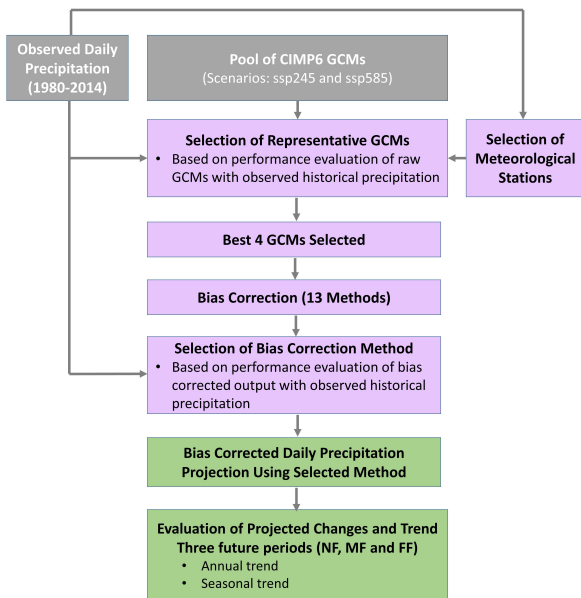


**Figure 2:** Methodological flowchart of this study

### 3.1 Data

### 3.1.1 Observed daily precipitation data

Observed historical daily precipitation data at the stations within the GRB was collected from DHM for the baseline period of 1980 to 2014.

### 3.1.2 Climate model datasets

CMIP6-GCMs model outputs were collected from World Climate Research Programme (WCRP) website <https://esgfnode.llnl.gov/search/cmip6/> for daily precipitation data. GCMs were selected on the criteria of nominal resolution of 100km or less. CMIP6-GCMs (along with their spatial resolutions) as given in Table 1.

**Table 1:** Initial pool of GCMs used

S. No.	Model name	Latitude resolution	Longitude resolution
1	MRI-ESM2-0	1.1215	1.125
2	BCC-CSM2-MR	1.1215	1.125
3	INM-CM4-8	1.5	2
4	INM-CM5-0	1.5	2
5	NorESM2-MM	0.9424	1.25
6	CMCC-CM2-SR5	0.9424	1.25
7	MPI-ESM1-2-LR	1.8653	1.875
8	MPI-ESM1-2-HR	0.9351	0.9375
9	ACCESS-ESM1-5	1.5	1.875
10	ACCESS-CM2	1.25	1.875
11	EC-Earth3-Veg	0.7018	0.7031
12	EC-Earth3	0.7018	0.7031

## 3.2 Methodology

### 3.2.1 Selection of scenarios

The middle-of-the-road approach combined with the reasonable end of the emission scenario (SSP245) was used for the study. In addition, the fossil-fueled development approach combined with the high end of emission scenario (SSP585) was also used as the SSPs to cover, in general, the low to the high end of emission scenario and wider SSPs.

### 3.2.2 Selection of study period

The reference period for the study is taken as 1980-2014, and the future period is divided into three categories; near future (NF: 2021-2046), mid-future (MF: 2047-2073), and far-future (FF: 2074-2100).

### 3.2.3 Selection of meteorological stations

The meteorological stations for climatic projection were screened based on two steps: (i) Initial screening by data quality assessment where stations with missing data less than 10% were filtered (total 44 stations). Then, (ii) the second stage of screening to reduce the number of stations without compromising the spatial coverage of the station over the basin (total 25 stations shown in Figure 1).

### 3.2.4 Selection of representative GCMs

The selection of representative GCMs was based on evaluating the past performance by comparing the performance of precipitation projection made by the GCMs with the baseline observed data from 1980 to 2014. For quantifying the performance, the metrics used are Nash-Sutcliffe efficiency (NSE), the ratio of root mean square error to standard deviation (RSR), and percentage bias (PBIAS). The performance metrics of each model at all of the selected 25 stations

were computed and converted into arbitrary performance ratings based on Table 2. Based on the average of combined ratings of all metrics overall selected stations using a pool of twelve GCMs, the GCMs were ranked, and the best four GCMs Table 3 were selected.

**Table 2:** Performance rating criteria

Performance	NSE	RSR	PBIAS	Rating
Very Good	0.75 < NSE ≤ 1.00	0.00 < RSR ≤ 0.50	PB < 10	5
Good	0.65 < NSE ≤ 0.75	0.50 < RSR ≤ 0.60	10 ≤ PB < 15	4
Satisfactory	0.50 < NSE ≤ 0.65	0.60 < RSR ≤ 0.70	15 ≤ PB < 25	3
Unsatisfactory	0.4 < NSE ≤ 0.5	0.70 < RSR ≤ 0.80	25 ≤ PB < 35	2
Poor	NSE ≤ 0.4	RSR > 0.80	PB ≥ 35	1

**Table 3:** GCM selection based on average rating

GCM	Rating	GCM	Rating
MRI-ESM2-0	1.33	<i>MPI-ESM1-2-LR</i>	<b>2.32</b>
BCC-CSM2-MR	1.99	<i>MPI-ESM1-2-HR</i>	<b>2.41</b>
INM-CM4-8	2.31	ACCESS-ESM1-5	2.13
INM-CM5-0	2.11	ACCESS-CM2	1.20
NorESM2-MM	1.97	<i>EC-Earth3-Veg</i>	<b>2.42</b>
CMCC-CM2-SR5	1.95	<i>EC-Earth3</i>	<b>2.32</b>

### 3.2.5 Downscaling and bias correction

Data from climate models data often present biases compared to the observed data and needs to be downscaled and bias-corrected. Several statistical methods have been developed for correcting biases. In this paper, GCMs are statistically downscaled and bias-corrected using qmap package [15] using different methods [16] listed below:

- i. Bernoulli Exponential
- ii. Bernoulli Gamma
- iii. Bernoulli Weibull
- iv. Bernoulli Log-normal
- v. Exponential Asymptote
- vi. Exponential Asymptote x0
- vii. Linear Transformation
- viii. Power Transformation
- ix. Power x0 Transformation
- x. Scale Transformation
- xi. Non-parametric Quantile Mapping
- xii. Non-parametric Robust Quantile Mapping
- xiii. Smoothing Spline

### 3.2.6 Selection of bias correction method

The best-suited bias correction method for this area was selected by comparing the performance of bias-corrected precipitation from the selected GCMs

at 25 stations with the baseline observed data from 1980 to 2014. The metrics used for quantifying the performance are NSE, RSR and PBIAS, similar to Section 3.2.4. *Non-parametric robust quantile mapping* performed best, and bias-corrected future projection was made using this method for two climate scenarios (SSP245 and SSP585).

### 3.2.7 Evaluation of projected changes and trend

Projected future precipitation for two selected scenarios of SSP245 and SSP585, based on selected four GCMs and a multi-model ensemble (MME) was then used to assess the impact of climate change on three future periods (near future-NF, mid future-MF and far future-FF). The impacted is assessed by comparing the changes in future precipitation with reference to the baseline precipitation of 1980-2014 duration and the likely trend in the three future periods were also evaluated using Mann Kendall trend test along with Sen's slope estimator [17].

## 4. Results and Discussion

### 4.1 Projected changes in average annual precipitation

Time series of projected precipitation with a daily temporal resolution, at selected 25 meteorological stations, using four different GCMs is the primary output of the downscaling and bias correction process. Figure 3 shows the yearly accumulated precipitation as projected from MME of four GCMs and for two different scenarios for one station (station-823), for all three future periods (NF, MF & FF). Historical average annual precipitation for the baseline period of 1980-2014 is shown in Figure 4.

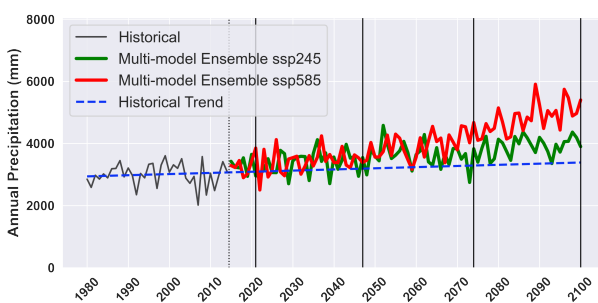


**Figure 3:** Historical versus projected annual precipitation at station-823

The change in future precipitation in three future periods NF, MF & FF for scenario SSP245 is shown in Figure 5.

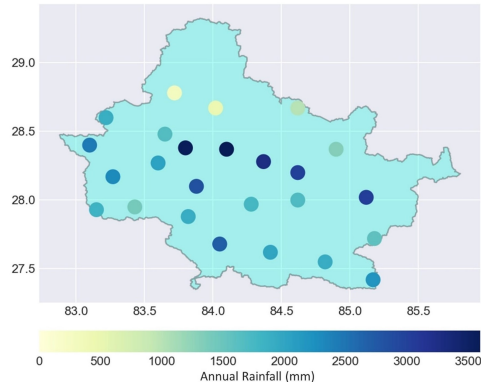


**Figure 4:** Spatial distribution of station-wise historical average annual precipitation of Gandaki River basin

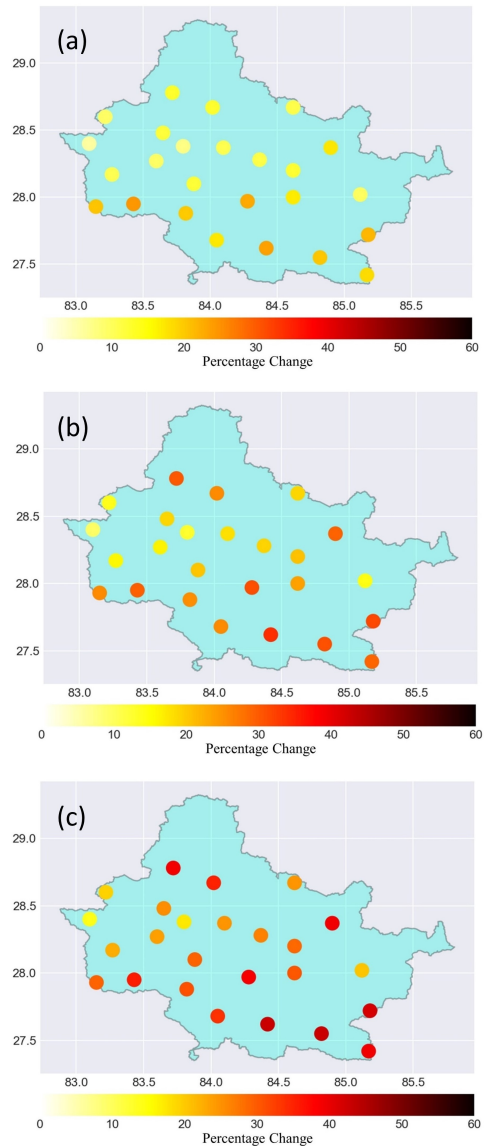


**Figure 5:** Projected % change in average annual precipitation in (a) NF, (b) MF, and (c) FF, under SSP245 with respect to the baseline period.

The multi-model ensemble of four GCMs for SSP245 indicated 7-32% increase in annual precipitation NF and 18-45% increase in FF for SSP245 scenario across the selected 25 stations.

The change in future precipitation in three future periods NF, MF, & FF under SSP585 is shown in Figure 6. The multimodel ensemble of four GCMs indicated a 6-35% increase in NF and up to 42-110% increase in FF under SSP585 across the selected 25 stations.

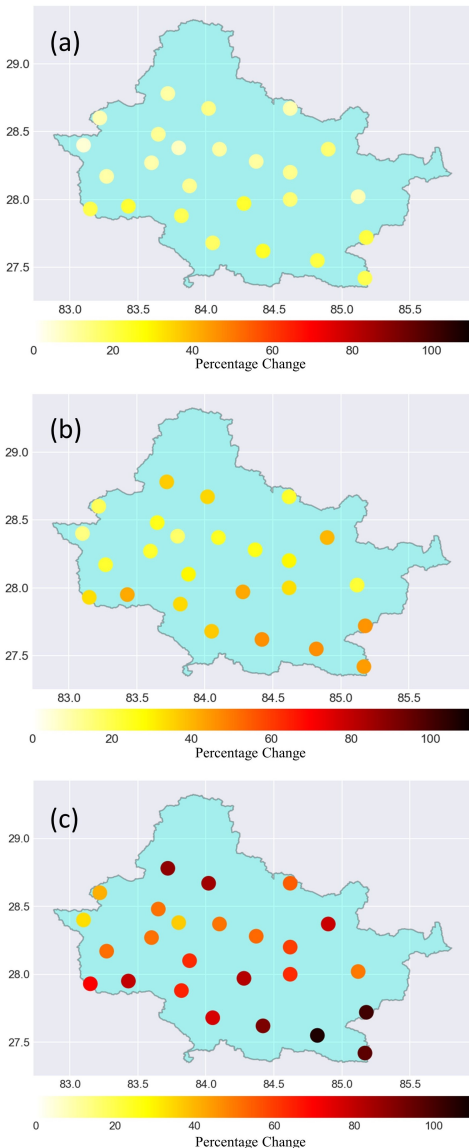


**Figure 6:** Projected % change in average annual precipitation in (a) NF, (b) MF, and (c) FF, under SSP585 with respect to the baseline period

#### 4.2 Seasonality of projected changes

The large size of the GRB warrants spatial heterogeneity in the projected precipitation. Future

precipitation at three representative stations spread across three physiographic regions within the basin to investigate the heterogeneity. The stations are st-806 (mountain region, masl = 3650m, location = Larke Samdo, Gorkha), st-802 (hilly region, masl = 823m, location = Khudi Bazar, Lamjung) and st-920 (Terai region, masl = 274m, location = Beluwa, Makwanpur).

At mountain station st-806, the monthly and seasonal changes in precipitation under SSP245 and SSP585 are presented in Figure 7 and Figure 8 respectively. Under SSP245, average annual precipitation are projected to increase by 11%, 19% and 25% during the NF, MF, and FF, respectively. On a seasonal scale, change in monsoon precipitation is expected to be 21%, 33%, and 48% in NF, MF, and FF, respectively. Similarly, change in post-monsoon precipitation is projected to be -12%, -1%, and 2%, change in winter precipitation will be -8%, -10%, and -16%, and change in pre-monsoon precipitation will be 12%, 16%, and 20% in NF, MF, and FF, respectively.

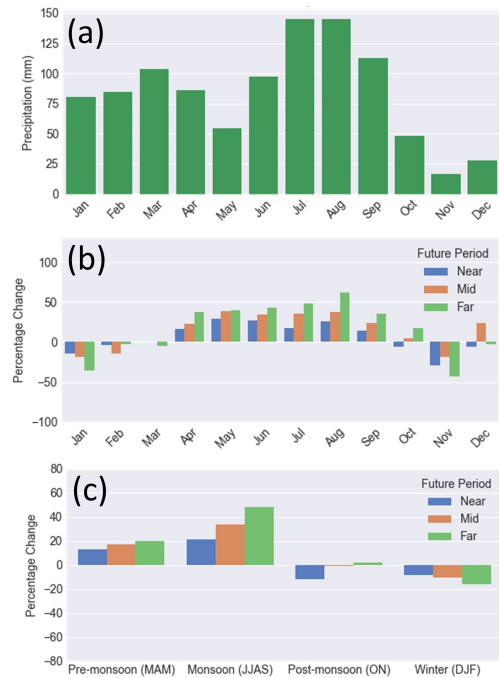


**Figure 7:** (a) Historical monthly precipitation, Change in (b) monthly and (c) seasonal precipitation, at mountain station-806 under SSP245

Under SSP585, average annual precipitation is projected to increase by 9%, 23%, and 54% in NF, MF, and FF. On a seasonal scale, change in monsoon precipitation is anticipated to be 21%, 47%, and 101% in NF, MF, and FF, respectively. Similarly, change in post-monsoon precipitation is expected to be 4%, 5%,

and 37%, change in winter precipitation will be -9%, -20%, and -24% and change in pre-monsoon precipitation will be 5%, 18%, and 29% in NF, MF, and FF, respectively.

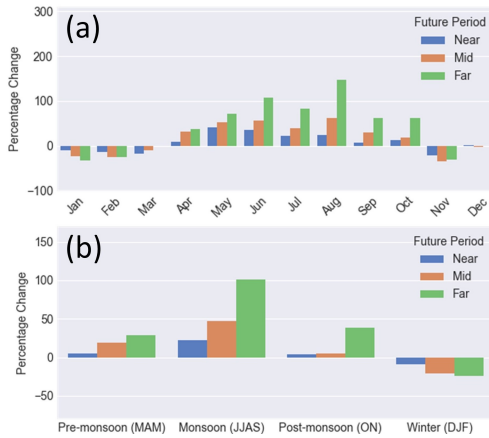


**Figure 8:** Change in (a) monthly and (b) seasonal precipitation, at mountain station-806 under SSP585

At hill station st-802, the monthly and seasonal changes in precipitation under SSP245 and SSP585 are presented in Figure 9 and Figure 10 respectively.

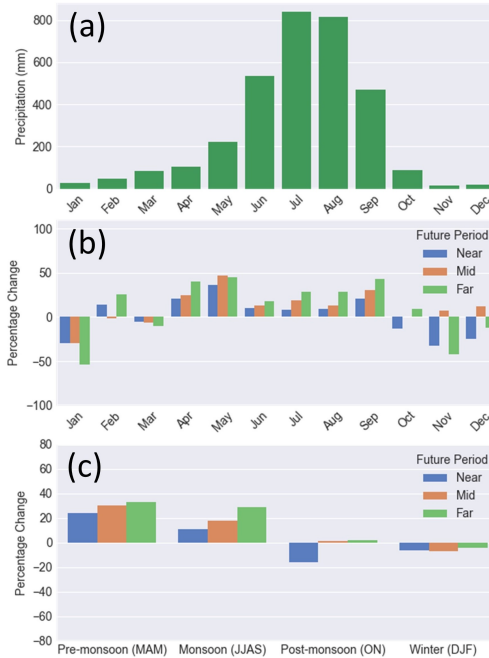


**Figure 9:** (a) Historical monthly precipitation, Change in (b) monthly and (c) seasonal precipitation, at hill station-802 under SSP245

Under SSP245, average annual precipitation is projected to increase by 11%, 19%, and 26% in NF, MF, and FF, respectively. On a seasonal scale, change in monsoon precipitation is expected to be 11%, 18%,

and 29% in NF, MF, and FF, respectively. Similarly, change in post-monsoon precipitation is projected to be -16%, 1%, and 2%, change in winter precipitation will be -6%, -7%, and -5%, and change in pre-monsoon precipitation will be 23%, 30%, and 33% in NF, MF, and FF, respectively. Under SSP585, average annual precipitation is projected to increase by 1%, 25%, and 53% in NF, MF, and FF, respectively. On a seasonal scale, change in monsoon precipitation is expected to be 12%, 27%, and 58% in NF, MF, and FF, respectively. Similarly, change in post-monsoon precipitation is expected to be 3%, 4%, and 38%, change in winter precipitation will be -9%, -23%, and -19%, and change in pre-monsoon precipitation will be 22%, 36% and 48% in NF, MF and FF, respectively.

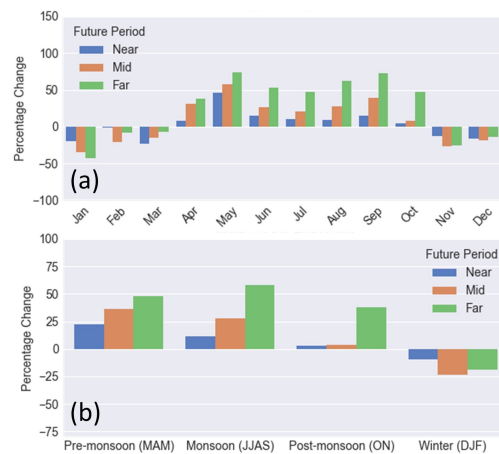


**Figure 10:** Change in (a) monthly and (b) seasonal precipitation, at hill station-802 under SSP585

At terai station st-920, the monthly and seasonal changes in precipitation under SSP245 and SSP585 are presented in Figure 11 and Figure 12 respectively. For SSP245, average annual precipitation are projected to increase by 20%, 31% and 43% in NF, MF and FF. Change in monsoon precipitation is expected to be 22%, 34% and 45% in NF, MF and FF based on multi-model ensemble. Change in post-monsoon precipitation is expected to be -6%, 11% and 35%, change in winter precipitation is -23%, -13% and -33%, and change in pre-monsoon precipitation is 47%, 35% and 48% in NF, MF and FF. For SSP585 scenario, average annual precipitation are projected to increase by 21%, 46% and 106% in NF, MF and FF. Change in monsoon precipitation is expected to be 23%, 51% and 45% in NF, MF and FF based on multi-model ensemble. Change in post-monsoon precipitation is expected to be 11%,

41% and 35%, change in winter precipitation is -11%, -30% and -33%, and change in pre-monsoon precipitation is 36%, 54% and 49% in NF, MF and FF.

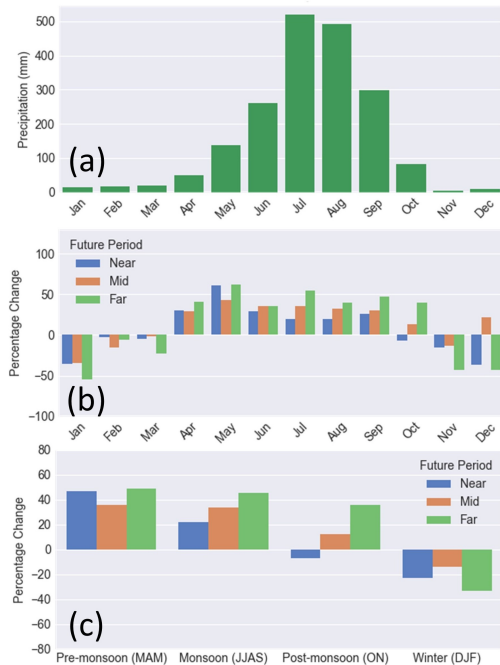


**Figure 11:** (a) Historical monthly precipitation, Change in (b) monthly and (c) seasonal precipitation, at terai station-920 under SSP245

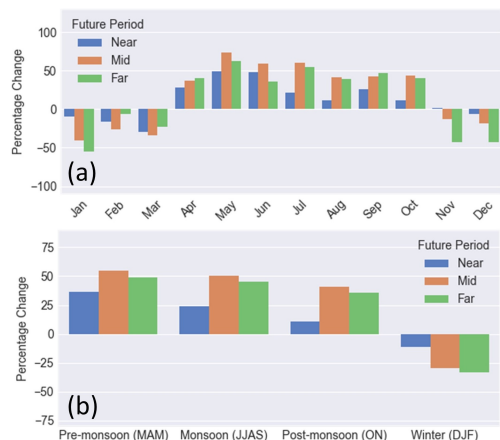


**Figure 12:** Change in (a) monthly and (b) seasonal precipitation at terai station-920 under SSP585

### 4.3 Projected future trends in precipitation

The change in precipitation, if any, brought by the change in climatic scenario can be ascertained after assessing the historical trend in precipitation i.e. by comparing the historical trend with the trend of future projection under climate scenarios. Figure 4 shows historical trend of annual precipitation (based on

Mann-Kendall test with Sen's slope) in all selected 25 stations. The trend is indicated as constant if the Sen's slope indicated change over any considered period is greater than -5% and less than 5% of baseline precipitation. Trend is indicated as slightly increasing if increase is less than 10% increasing if increase is greater than or equal to 10%, slightly decreasing if decrease is less than 10% and decreasing if decrease is less than or equal to 10%.

The spatial plot shows no definite trend in precipitation over the basin in the historical period, and the trend on most stations is not significant. Figure 3 indicates that the annual precipitation will rise in the future period at station 823 under both SSPs, more pronounced under SSP585 than SSP245. Plots at other stations indicate the same pattern in the future period.

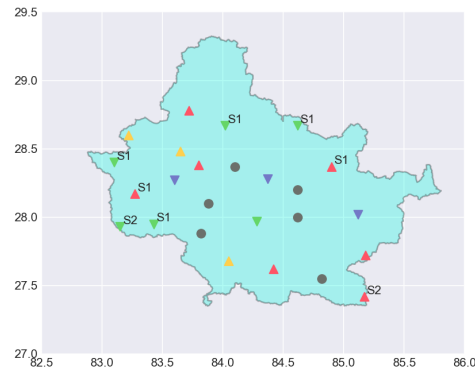


**Figure 13:** Historical trend of annual precipitation (red  $\Delta$  = rise, orange  $\Delta$  = slight rise, O= no trend, blue  $\nabla$ = slight decrease, green  $\nabla$  =decrease, S1 = 5% significance level, S2 = 10% significance level)

Trend analysis was performed for all selected 25 stations for annual precipitation in future for three future periods (NF, MF & FF) under SSP245 and SSP585. As indicated by the multimodel ensemble under SSP245, the trend across the majority of the stations is rising (with varying levels of significance) for all three future periods (Figure 14). Likewise, the trend under SSP585 for most of the stations also indicated a rise across all three future periods, with a trend significant on the majority of the stations (Figure 15).

The results from this study fall in line with the findings obtained on adjacent Koshi, Karnali basin and other smaller basins of Nepal that the precipitation is set to change in future with gradual increase in precipitation over the long run to be more likely.

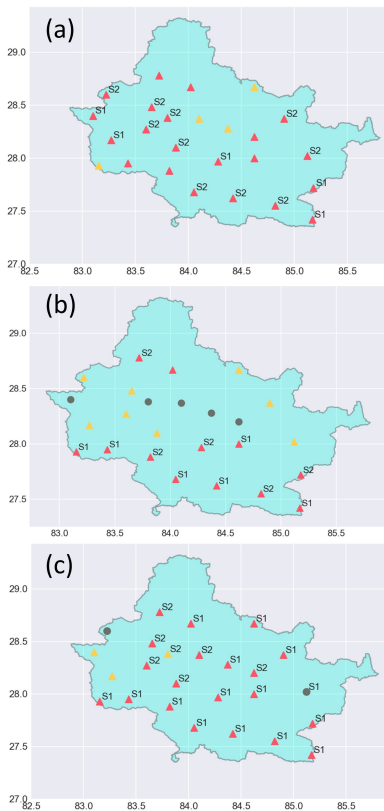


**Figure 14:** Trend of annual precipitation in (a) NF, (b) MF and (c) FF, under SSP245

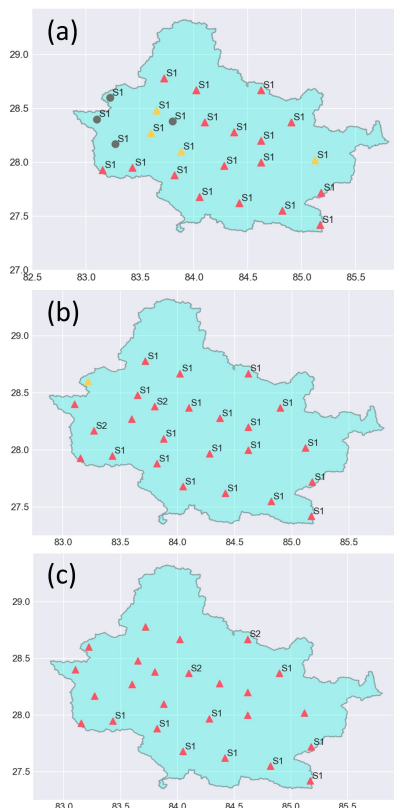


**Figure 15:** Trend of annual precipitation in (a) NF, (b) MF and (c) FF, under SSP585

## 5. Conclusion

The selection of representative climate models and an appropriate bias correction method is vital for precipitation projection. The past performance approach is widely used for selecting climate models, and the multimodel ensemble informs inter-model uncertainties in the projection. This study indicates the selected four GCMs (EC-Earth3-Veg, MPI-ESM1-2-HR, MPI-ESM1-2-LR, EC-Earth3) are suitable for representing future precipitation in the GRB. Furthermore, among various bias correction techniques, non-parametric robust quantile mapping is found to be the best-suited for correcting biases in CMIP6 GCM outputs in the GRB.

Historical precipitation had no definite trend over the considered baseline period. However, the rising trend is observed in annual precipitation across all three future periods and both climate scenarios of SSP245 and SSP585. Future average annual precipitation is projected to increase by 7-32% during the NF and 18-45% during the FF under SSP245, while 6-35% increase during the NF and 42-110% increase during the FF under SSP585. The intra-annual variability exists in the projected precipitation as indicated by the projected decrease from November till March and then increase during April-October in all three physiographic regions. Pre-monsoon and monsoon seasons are projected to get wetter, whereas post-monsoon and winter seasons will get drier.

The projected precipitation can be used in predicting future hydrology, assess the impact of climate change on future water availability and consequent planning and management of water resources in future.

## References

- [1] Christopher B Field and Vicente R Barros. *Climate change 2014—Impacts, adaptation and vulnerability: Regional aspects*. Cambridge University Press, 2014.
- [2] Dibesh Khadka, Mukand S Babel, Sangam Shrestha, and Nitin K Tripathi. Climate change impact on glacier and snow melt and runoff in tamakoshi basin in the hindu kush himalayan (hhk) region. *Journal of Hydrology*, 511:49–60, 2014.
- [3] Sangam Shrestha and Aung Ye Htut. Modelling the potential impacts of climate change on hydrology of the bago river basin, myanmar. *International Journal of River Basin Management*, 14(3):287–297, 2016.
- [4] P-A Versini, L Pouget, S McEnnis, E Custodio, and I Escaler. Climate change impact on water resources availability: case study of the llobregat river basin

- (spain). *Hydrological Sciences Journal*, 61(14):2496–2508, 2016.
- [5] Keywan Riahi, Detlef P Van Vuuren, Elmar Kriegler, Jae Edmonds, Brian C O’neill, Shinichiro Fujimori, Nico Bauer, Katherine Calvin, Rob Dellink, Oliver Fricko, et al. The shared socioeconomic pathways and their energy, land use, and greenhouse gas emissions implications: An overview. *Global environmental change*, 42:153–168, 2017.
- [6] Rupak Rajbhandari, Arun Bhakta Shrestha, Santosh Nepal, and Shahriar Wahid. Projection of future climate over the koshi river basin based on cmip5 gcms. *Atmospheric and Climate Sciences*, 6(2):190–204, 2016.
- [7] A Khadka, LP Devkota, and RB Kayastha. Impact of climate change on the snow hydrology of koshi river basin. *Journal of Hydrology and Meteorology*, 9(1):28–44, 2015.
- [8] Vaskar Dahal, Narendra Man Shakya, and Rabin Bhattacharai. Estimating the impact of climate change on water availability in bagmati basin, nepal. *Environmental Processes*, 3(1):1–17, 2016.
- [9] Vishnu Prasad Pandey, Sanita Dhaubanjar, Luna Bharati, and Bhesh Raj Thapa. Hydrological response of chamelia watershed in mahakali basin to climate change. *Science of the Total Environment*, 650:365–383, 2019.
- [10] Vishnu Prasad Pandey, Sanita Dhaubanjar, Luna Bharati, and Bhesh Raj Thapa. Spatio-temporal distribution of water availability in karnali-mohana basin, western nepal: Hydrological model development using multi-site calibration approach (part-a). *Journal of Hydrology: Regional Studies*, 29:100690, 2020.
- [11] Laxmi Prasad Devkota and Dhiraj Raj Gyawali. Impacts of climate change on hydrological regime and water resources management of the koshi river basin, nepal. *Journal of Hydrology: Regional Studies*, 4:502–515, 2015.
- [12] Santosh Kaini, Santosh Nepal, Saurav Pradhananga, Ted Gardner, and Ashok K Sharma. Impacts of climate change on the flow of the transboundary koshi river, with implications for local irrigation. *International Journal of Water Resources Development*, pages 1–26, 2020.
- [13] Rocky Talchabhadel. Observations and climate models confirm precipitation pattern is changing over nepal. *Jalawaayu*, 1(1):25–46, 2021.
- [14] Ramesh Chhetri, Vishnu P Pandey, Rocky Talchabhadel, and Bhesh Raj Thapa. How do cmip6 models project changes in precipitation extremes over seasons and locations across the mid hills of nepal? *Theoretical and Applied Climatology*, pages 1–18, 2021.
- [15] Lukas Gudmundsson. *qmap: Statistical transformations for post-processing climate model output*, 2016. R package version 1.0-4.
- [16] L. Gudmundsson, J. B. Bremnes, J. E. Haugen, and T. Engen-Skaugen. Technical note: Downscaling rcm precipitation to the station scale using statistical transformations - a comparison of methods. *Hydrology and Earth System Sciences*, 16(9):3383–3390, 2012.
- [17] T Salmi, A Määttä, P Anttila, T Ruoho-Airola, and T Amnell. Makesens 1.0. mann-kendall test and sen’s slope estimates for the trend of annual data. publications on air quality, no. 31, finnish meteorological institute. 2002.